ChemPubSoc Europe

DOI: 10.1002/open.201900215

Open Access ChemistryOPEN Full Papers

Mechanistic Insights into a Sustainable Mechanochemical Synthesis of Ettringite

Julia Stroh,*[a] Torvid Feiler,[a] Naveed Zafar Ali,[b] Manuel E. Minas da Piedade,[c] and Franziska Emmerling*[a]

Mechanochemistry offers an environmentally benign and facile synthesis method for a variety of cement paste constituents. In addition, these methods can be used to selectively tune the properties of cement components. The mineral ettringite is an important component of cementitious materials and has additional technological potential due to its ion exchange properties. Synthesis of ettringite via mechanochemistry is an environmentally friendly alternative to conventional wet-chemical synthesis established in industry. This contribution explores the mechanism of a two-step mechanochemical synthesis of ettringite, which was previously found to greatly improve the reaction conversion as compared with one-pot synthesis. The crystallinity of $Al(OH)_3$ was found to decrease during the first stage of this mechanochemical synthesis. This was correlated to a significant decrease in the particle size of $Al(OH)_3$ in this stage. No other significant changes were found for the other components, suggesting that mechanochemical activation of $Al(OH)_3$ is responsible for the enhanced formation of ettringite by the two-step approach. The environmentally friendly approach developed for ettringite synthesis offers a versatile synthetic strategy, which can be applied to synthesise further cementitious materials.

1. Introduction

The mineral ettringite $[Ca_3Al(OH)_6]_2 \cdot (SO_4)_3 \cdot 26H_2O$ is a key constituent in cement-based construction materials and is considered an integral part of the cementitious matrix.[1–6] The crystal structure of ettringite consists of columns of alternating calcium and aluminium polyhedra (Figure 1). The channels between the columns contain sulphate anions, which can be exchanged by other acidic anions.[7–10] Calcium or aluminium can be replaced by other metal cations incorporated into the structure.[11–19] This ion exchange ability and some other unique properties have extended the interest in ettringite well beyond construction industries. For example, ettringite properties are fundamental to the use of cement-based materials for the storage of hazardous waste,[20] paper and plastic manufacturing,[21] and for the novel developments of the adsorption-based treatment of wastewater and environmental remediation.[8,11,22–25]

Conventional ettringite syntheses are time-, energy-, and water-consuming and produce large quantities of chemical waste.[21] Furthermore, the preparation of ettringite precursors is accompanied by release of significant quantities of CO_2. This

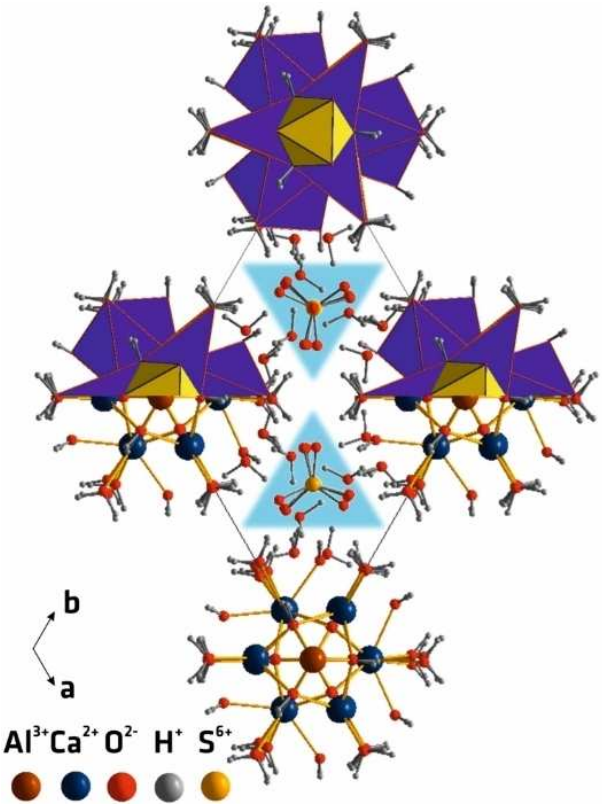

Figure 1. Crystal structure of ettringite showing (dark blue) calcium polyhedra, (yellow) aluminium octahedrons and (light blue) sulphate anions in channels. Structural water is also observed in the channels.[26]

[a] Dr. J. Stroh, T. Feiler, Dr. F. Emmerling
Federal Institute for Materials Research and Testing (BAM), Richard-Willstätter-Straße 11, 12489 Berlin, Germany
E-mail: julia.stroh@bam.de
franziska.emmerling@bam.de
[b] Dr. N. Zafar Ali
National Center for Physics, Quaid-i-Azam University Campus, Islamabad, Pakistan
[c] Prof. M. E. Minas da Piedade
Centro de Química e Bioquímica e Centro de Química Estrutural, Faculdade de Ciências, Universidade de Lisboa, 1749-016 Lisboa, Portugal

Supporting information for this article is available on the WWW under https://doi.org/10.1002/open.201900215

© 2019 The Authors. Published by Wiley-VCH Verlag GmbH & Co. KGaA. This is an open access article under the terms of the Creative Commons Attribution Non-Commercial NoDerivs License, which permits use and distribution in any medium, provided the original work is properly cited, the use is non-commercial and no modifications or adaptations are made.

© 2019 The Authors. Published by Wiley-VCH Verlag GmbH & Co. KGaA

owes to the burning of $CaCO_3$ as the source of calcium. Ettringite production would, therefore, benefit greatly from the development of new synthetic pathways, economically viable and fulfilling current ecological requirements.

Typical routes to ettringite formation are listed in Table 1. In cementitious systems, ettringite forms during the hardening process according to Eq. 1,[5,27,28] and this reaction can be performed in small scale under laboratory conditions. Eq. 1 requires, however, the formation of tricalcium aluminate $Ca_3Al_2O_6$, which is prepared by repeated burning of $CaCO_3$ and Al_2O_3 at 1400 °C.[5,29,30] This step produces at least three times more CO_2 than ettringite. The synthesis of ettringite described by Fridrichová et al. (2) requires preparation of the mineral ye'elimite $Ca_4Al_6O_{12}(SO_4)$ by burning of $CaCO_3$, Al_2O_3 and $CaSO_4 \cdot 2H_2O$ at up to 1250 °C for 5 h.[31] Further wet-chemical syntheses from pure reactants can be performed according to Eq. 3 and Eq. 4. All these syntheses include stirring of the reactant-containing suspension, filtration of the suspension after stirring, washing, and prolonged drying of the reaction product.[29,31] Consequently, the synthetic procedures require hours to days and must be conducted under inert atmosphere or in special (e.g. sucrose) environments.[7,32] These precautions prevent possible decomposition of ettringite in the presence of CO_2.[13,33] Ettringite can be further obtained as a by-product of the treatment of industrial waste water with $Ca_{12}Al_{14}O_{33}$.[34] However, product purification is still required. An alternative synthesis route has been reported, in which ultrasound treatment of the reactant-bearing suspension accelerates ettringite precipitation.[13] Although the ultrasonication significantly reduces the reaction time, the environmental impact due to the separation of ettringite from the mother suspension and from the side product remains. Thus, an improved, ready-to-use and environmentally benign synthesis of ettringite, which is fast, reduces CO_2 emissions, as well as energy and water consumption, is still lacking.

Table 1. Some possible ettringite formation routes.

Eq.	Reaction
1	$Ca_3Al_2O_6 + 3\ CaSO_4 \cdot 2H_2O + 26\ H_2O \rightarrow [Ca_3Al(OH)_6]_2 \cdot (SO_4)_3 \cdot 26H_2O$[5,27,28]
2	$6\ Ca_4Al_6(SO_4)O_{12} + 160\ H_2O \rightarrow 2\ [Ca_3Al(OH)_6]_2 \cdot (SO_4)_3 \cdot 26H_2O + 26\ Al(OH)_3 + 3\ Ca_4[Al(OH)_6]_2 \cdot (OH)_2 \cdot 12H_2O$[31]
3	$3\ Ca(OH)_2 + 2\ Al(OH)_3 + 3\ CaSO_4 \cdot 2H_2O + 20\ H_2O \rightarrow [Ca_3Al(OH)_6]_2 \cdot (SO_4)_3 \cdot 26H_2O$[35]
4	$Al_2(SO_4)_3 \cdot 18H_2O + 6\ CaO + 14\ H_2O \rightarrow [Ca_3Al(OH)_6]_2 \cdot (SO_4)_3 \cdot 26H_2O$[16,36]

Mechanochemistry is an effective solid-state approach for the rapid synthesis of materials in high yields.[25,35,37–58] Extensive reviews of mechanosyntheses are available,[49,59–62] highlighting their particular benefit of avoiding solvent waste. With respect to ettringite formation, these high-yield mechanochemical techniques promise to reduce solvent requirements, while further reducing necessary purification steps. Zhong et al. have studied the mechanochemical preparation of the ettringite precursor, which was later used to remove pollutants from wastewater by the formation of ettringite.[25] Other reports describe the mechanochemical formation of complex calcium-metal hydrates that are structurally related to ettringite.[25,42]

Recently, we elaborated the suitable strategy for the sustainable mechanochemical synthesis of ettringite.[35] The strategy included the neat pre-grinding of the solid reactants followed by the addition of the stoichiometric water amount. This grinding strategy is proved to be very effective, leading to 94 %$_{wt.}$ of the reaction conversion after a reaction time of 2 h. The product is a dry powder containing 94 %$_{wt.}$ ettringite, which is of the adequate quality for many industrial applications and waste water treatment.

Here, we explore the mechanistic details of ettringite synthesis by mechanochemistry. This work identifies the relative importance of mechanochemical activation of individual solid components on the rate and mechanism of ettringite formation. The reaction conversion is considerably influenced by the duration of the neat pre-grinding. The latter affects primarily the crystallinity of the solid reactants. The crystallinity of $Al(OH)_3$ lowers significantly during the grinding, whereas the crystallinities of $Ca(OH)_2$ and $CaSO_4 \cdot 2H_2O$ hardly change. Thereby, the decrease in crystallinity of $Al(OH)_3$ in the presence of $Ca(OH)_2$ is crucial for the achieving the high conversion of this mechanochemical reaction. The variations in the order of reactant mixing allowed us to identify solid reactants for which mechanochemical activation plays the most crucial role. This work therefore provides a new understanding of the two-step mechanochemical ettringite formation and paves the way to further improvement of the synthesis efficiency and its possible industrial implementation.

Experimental Section

The mechanosyntheses were carried out according to Eq. 3 (Table 1). The grinding experiments were performed in a vibratory ball mill Pulverisette 23 (Fritsch, Germany) at a frequency of 50 Hz. The syntheses were carried out using a 10 mL Perspex grinding jar and two zirconia balls (diameter 10 mm, weight 3 g) to exclude the incorporation of iron from the milling equipment into the ettringite structure.[35] Aluminium hydroxide $Al(OH)_3$ (Kraft, $\geq$99 %), calcium sulphate dihydrate $CaSO_4 \cdot 2H_2O$ (Bernd Kraft, $\geq$98 %), calcium hydroxide $Ca(OH)_2$ (Sigma-Aldrich, $\geq$96 %) and water (MilliQ, 18.2 MΩ·cm) were used as reactants in the stoichiometric amounts according to Eq. 3. Variations of the grinding experiments included one-, two-, and three-step processes (Figure 2):

1 one-step syntheses: all four reactants were added into the jar and ground together;
2 two-step syntheses: Step 1: neat pre-grinding of dry reactants (gradual increase of the grinding duration from 15 to 120 min in 15 min steps). Step 2: the delayed addition of water and further grinding for 30 min;
3 three-step syntheses. Step 1: pairs of dry reactants were ground. Step 2: the third dry reactant was added, and the mixture was ground. Step 3: purified water was added to the mixture, and the mixture was ground. The details of these mechanosyntheses are summarized in Figure 3.

The aim of these three-step syntheses was to identify the intermediate steps of the mechanochemical ettringite formation

© 2019 The Authors. Published by Wiley-VCH Verlag GmbH & Co. KGaA

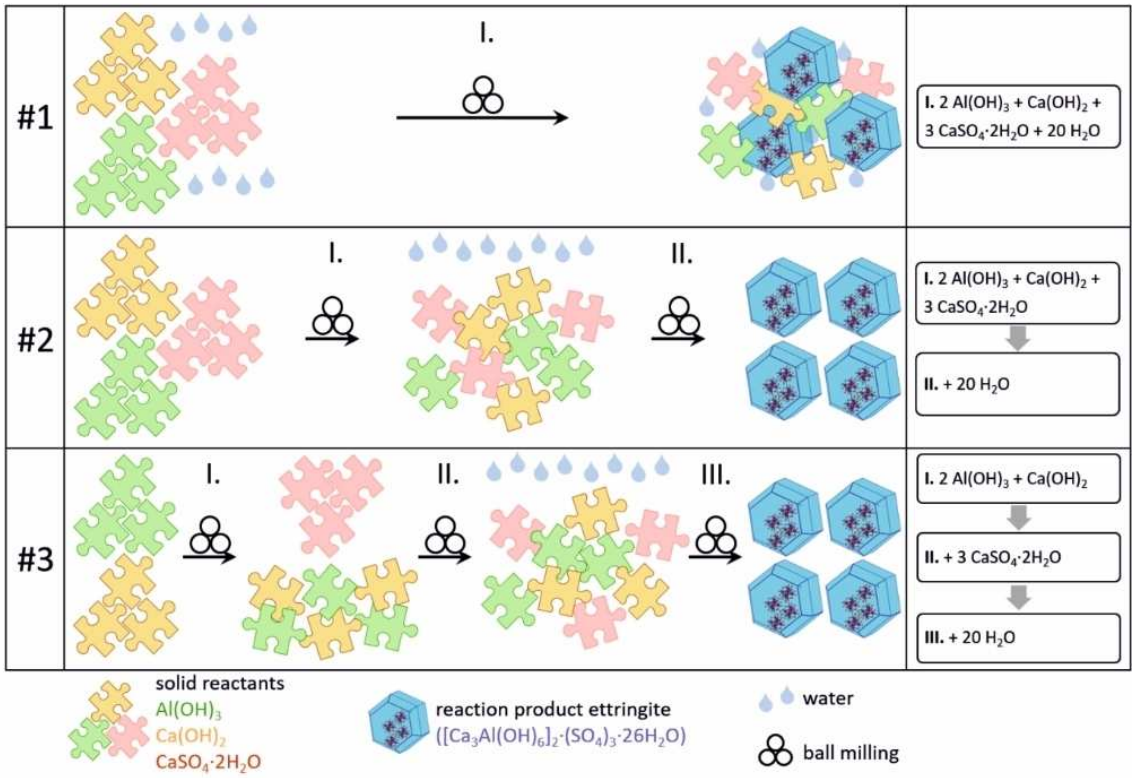

Figure 2. Scheme of the mechanosyntheses: (#1) one-step wet grinding; (#2) two-step grinding consisting of neat pre-grinding and wet grinding; (#3) three-step grinding consisting of two partial neat pre-grinding steps and wet grinding, exemplarily shown for one mechanosynthesis in the right column.

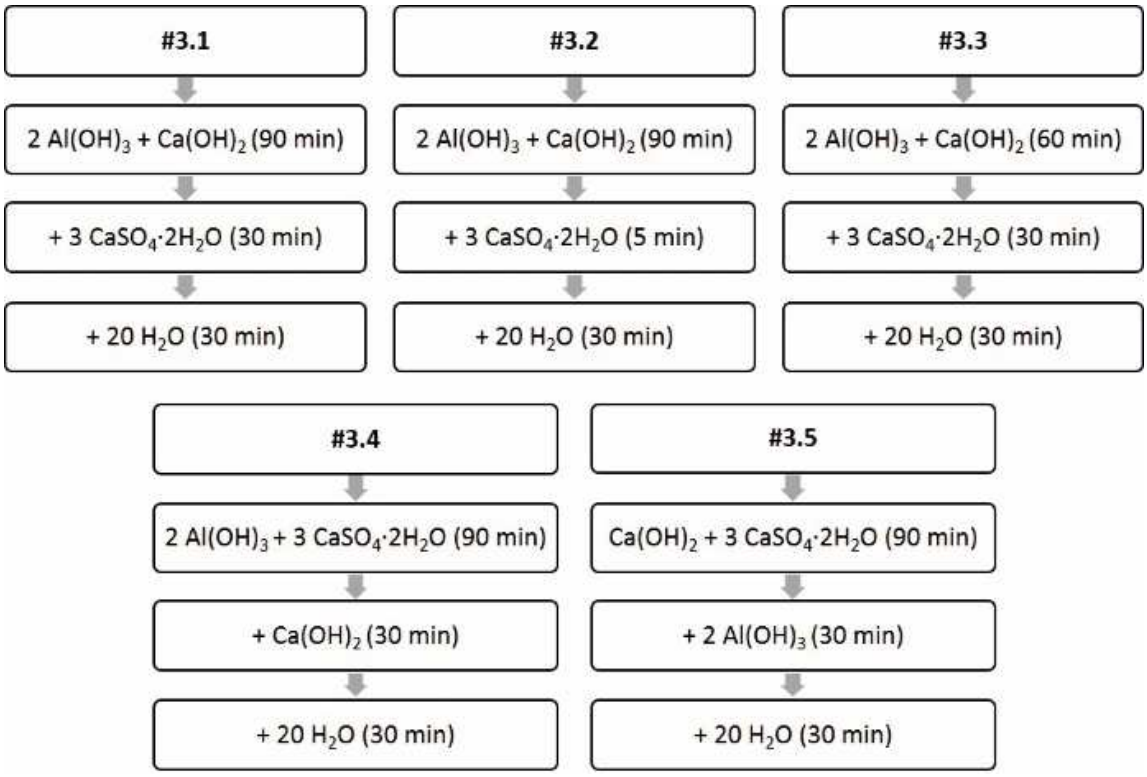

Figure 3. Schemes of the three-step mechanosyntheses (#3 in Figure 2). The duration of grinding after reactant addition is specified in brackets. The quantity of each reactant was calculated based on the reaction stoichiometry (Eq. 3, Table 1).

© 2019 The Authors. Published by Wiley-VCH Verlag GmbH & Co. KGaA

based on the products of the mechanochemical treatment of each reactant pairs. The durations of the Steps 1–3 are partly varied considering the grinding durations of the two-step syntheses. When varying the grinding time, we investigated potential effects of the grinding duration of individual reactant pairs on the intermediate formation.

The reaction products were analysed by powder X-ray diffraction on the Bragg-Brentano diffractometer D8 Advance (Bruker AXS, Germany) equipped with a LYNXEYE XE–T detector. The copper radiation source was operated at 40 keV and 40 mA. The samples were mounted in identical plate sample holders and measured with the step size of 0.02 ° and the measurement duration of the 2 s/step. To enable the direct comparison between the diffractograms and the calculated peak areas for the different samples without further normalization, all acquired diffractograms were reduced with respect to background using DIFFRAC.EVA V4.2 software (Bruker AXS, Germany) with curvature value 1.0 and the threshold value of 1.0. The amount of ettringite formed in the time-dependent two-step mechanosynthesis (#2) was assessed by calculation of the peak area of the (1 0 0) reflection at 9.09 ° 2θ ($Cu_{K\alpha1}$). The absolute peak area was calculated using numerical integration based on the trapezoidal calculation of the integral between 8.5 ° and 9.5 ° 2θ as implemented in Origin 2018G Software (OriginLab Corporation, USA). The crystallinity and the crystallite size of the samples were calculated using DIFFRAC.EVA V4.2 software. The calculation of the crystallinity for the individually ground reactants was based on the ratio of the reduced diffractogram area to its global area. The crystallite size of ettringite was calculated according to the Scherrer equation[63–65] using full width at the half-maximum (FWHM) of the (1 0 0) ettringite reflection. The particle size for the intermediate mixtures from the two-step syntheses (#2) was analysed by the laser granulometric analysis (Mastersizer S Vers. 2.18, Malvern Instruments Ltd, UK) after the suspending of the powder samples in isopropanol.

2. Results and Discussion

The product of the one-step mechanosynthesis was obtained as a damp, clay-like material. In the diffraction pattern shown in Figure 4, reflections of the reactants and product ettringite can be seen. The composition of this mixture indicates that only a small part of the starting materials reacted to the ettringite. Quantitative Rietveld refinement indicates that only 34 %$_{wt.}$ ettringite is present in the final mixture.[35] Residual moisture of the resulting mixture after 2 h grinding was the first evidence of an incomplete reaction, since the molar amount of water in the mixture should be entirely incorporated into the structure of ettringite.

In the two-step approach, solid reactants $Al(OH)_3$, $Ca(OH)_2$ and $CaSO_4 \cdot 2H_2O$ were ground under neat conditions for 90 min. In this case, no ettringite formation was observed. Water was subsequently added to the mixture, and the grinding continued for further 30 min. The resulting product contains 94 %$_{wt.}$ ettringite, as evidenced by quantitative Rietveld refinement.[35] Thus, the conversion obtained in the two-step mechanosynthesis is considerably higher than the conversion in the one-step mechanosynthesis, Figure 4.[35] We systematically increased the duration of the neat pre-grinding step from 15 min to 120 min to observe the influence of the grinding duration on the reaction conversion (Figure 5). The reflection of ettringite increases in intensity with prolonged neat pre-grinding. Figure 6 shows the dependence of the main peak area of ettringite from the grinding duration. From the calculations of the area of the (1 0 0) Bragg peak, the dependence of the amount of ettringite on the neat pre-grinding duration can be observed (Figure 6, right). Thus, the conversion is linked to the duration of the neat pre-grinding step. This dependence was

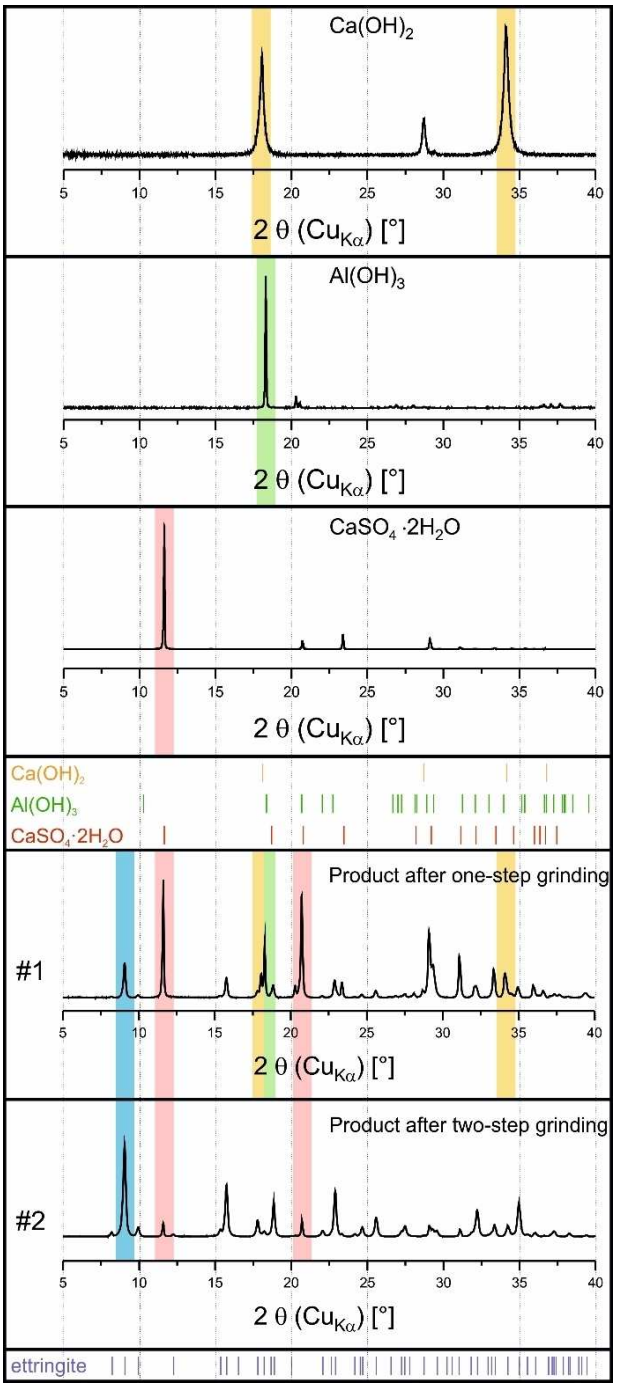

Figure 4. XRD data of the reactants and products of the one- and two-step syntheses. The main reflections are depicted in: blue – ettringite [$Ca_3Al(OH)_6]_2 \cdot (SO_4)_3 \cdot 26H_2O$, PDF 01-075-7554; red – $CaSO_4 \cdot 2H_2O$, PDF 00-074-1433; green – $Al(OH)_3$, PDF 01-074-1775; orange – $Ca(OH)_2$, PDF 00-044-1481.

© 2019 The Authors. Published by Wiley-VCH Verlag GmbH & Co. KGaA

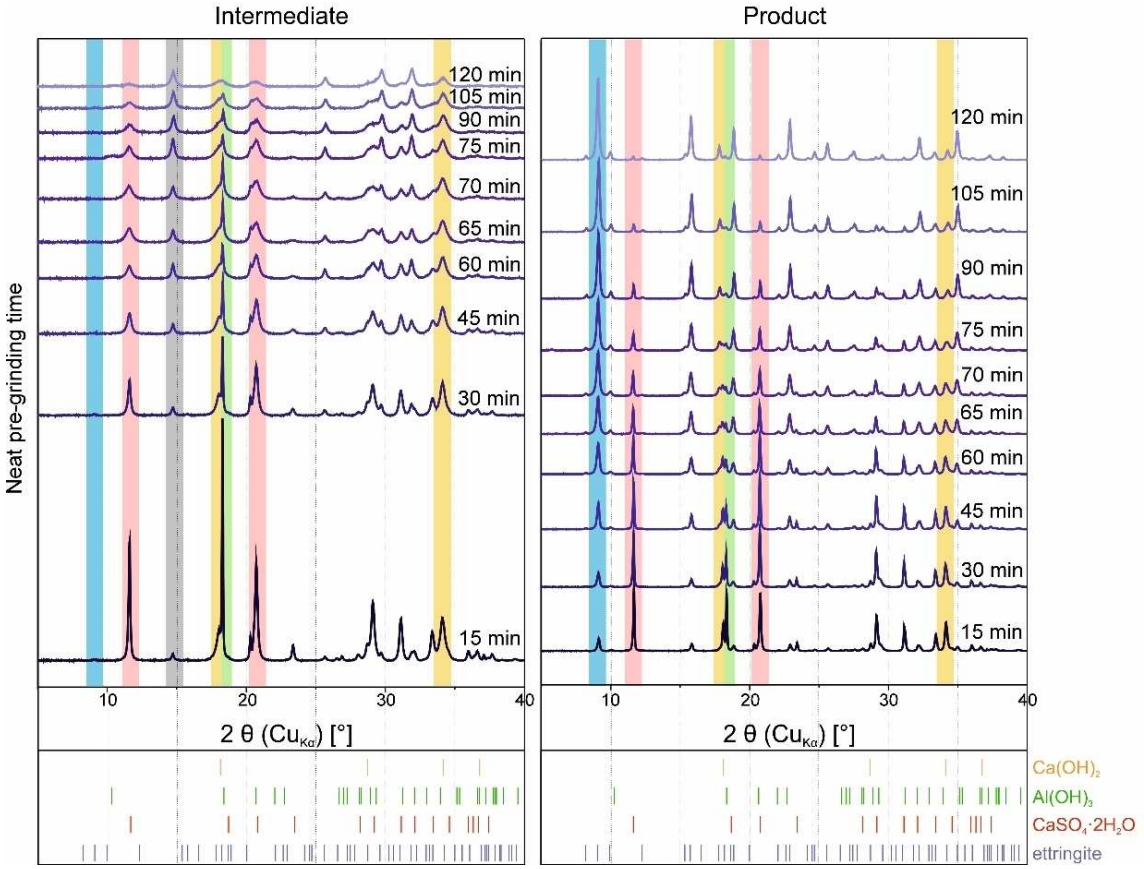

Figure 5. XRD data of the intermediate mixture and products obtained in the two-step mechanosyntheses (#2 in Figure 2) after variable neat pre-grinding time. The positions of the main reflections are depicted in: blue – ettringite $[Ca_3Al(OH)_6]_2\cdot(SO_4)_3\cdot 26H_2O$; red – $CaSO_4\cdot 2H_2O$; green – $Al(OH)_3$; orange – $Ca(OH)_2$.

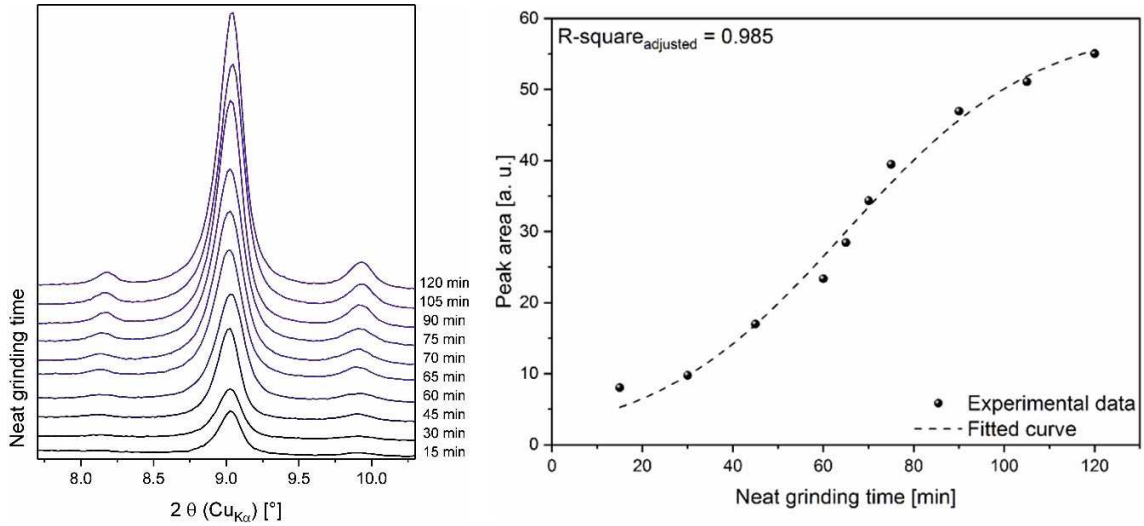

Figure 6. Dependence of the formed ettringite amount on the duration of the neat pre-grinding: left - development of the intensity of the main reflection; right – calculated peak area with related conversion values.

fitted using sigmoid function and shows a steep rise between 45 and 90 min of the neat grinding. The prolongation of the pre-grinding beyond 90 min leads to ca. 10% increase of the ettringite peak area, thus indicating the curve stagnation. The product achieved in the synthesis with neat pre-grinding duration of 120 min (2.5 h total synthesis time) contains 97%$_{wt.}$ ettringite according to the quantitative Rietveld refinement. Thus, the pre-grinding duration of 90 min seems to be the time needed to convert most of the reactants to ettringite (94%),

© 2019 The Authors. Published by Wiley-VCH Verlag GmbH & Co. KGaA

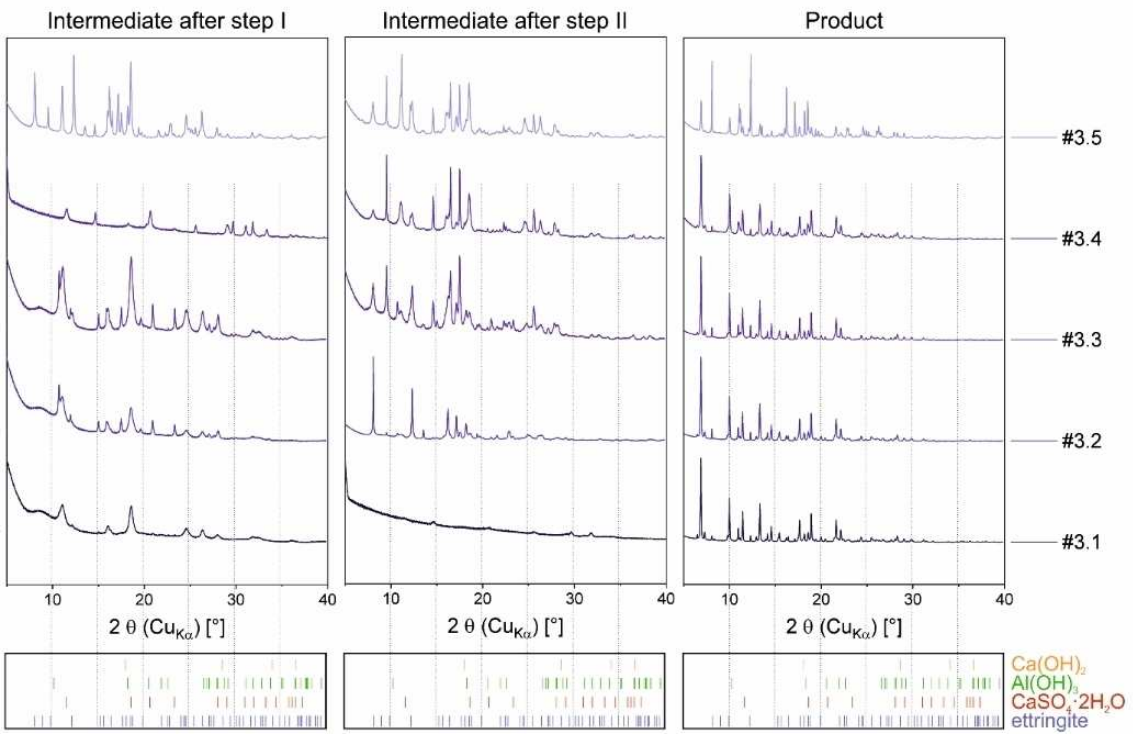

Figure 7. XRD data of the intermediates after steps I, II and of the final products of the three-step mechanosyntheses (#3). Positions of the main reflections are depicted in: blue - ettringite, $[Ca_3Al(OH)_6]_2\cdot(SO_4)_3\cdot 26H_2O$; red – $CaSO_4\cdot 2H_2O$; green – $Al(OH)_3$; yellow – $Ca(OH)_2$; grey – $CaSO_4\cdot 0.5H_2O$ (without bar code).

and an increase of the pre-grinding for further 30 min allows to achieve only 3% more of the aimed product.

XRD data of the pre-ground intermediate mixture are shown in Figure 5, left. The comparison indicates that prolonged neat pre-grinding leads to: (a) a marked decrease in the reflection intensities of the reactants, which suggests a significant mechanically induced reduction in particle size; (b) an overall decrease in crystallinity of the ground mixture (Figure S1). Since the intermediate mixture consists of several components, the decrease in its overall crystallinity can be related to changes in crystallinity in any of the mixture components. It can also be concluded that (c) the process is accompanied by the partial dehydration of gypsum to calcium sulphate hemihydrate $CaSO_4\cdot 0.5H_2O$ as indicated by a new peak at 17° 2theta. These findings were corroborated by the results of laser granulometric analysis, which showed that the neat grinding process does indeed lower the particle size of the resulting mixture (Figure S2).

To further evaluate the presence of grinding effects, we individually analysed the influence of the neat grinding duration on the crystallinity of each solid reactant (Figure S2). Prolonged milling of pure samples of $CaSO_4\cdot 2H_2O$ and $Ca(OH)_2$ did not show any notable changes in the diffraction patterns. Hence, it is unlikely that activation of these components is responsible for changes observed in the crystallinity of the mixture. In contrast, milling of $Al(OH)_3$ was met with significant decrease in scattering intensity of the resulting sample. It follows that milling of this compound leads to marked decrease in its crystallinity. Its crystallinity decreases substantially for grinding times up to 60 min, whereby at this point the total crystallinity decreases by ca. 60% and persists at this value if $Al(OH)_3$ is ground for further 60 min (Figure S2). Thus, significant reduction of the particle size and the activation occur during the prolonged mechanical treatment of $Al(OH)_3$. This mechanical activation of $Al(OH)_3$ during the neat pre-grinding of solid reactants in the two-step ettringite mechanosynthesis seems to play a significant role for the progress of the mechanochemical reaction. Some authors observed significant effects of mechanical treatment on $Al(OH)_3$ including the occurrence of structural defects and amorphization up to decomposition to Al_2O_3.[66–72]

A series of three-step mechanosyntheses were performed, according to procedures outlined in Figure 3. The XRD data of the intermediate mixtures produced in each step are shown in Figure 7, alongside XRD patterns for the respective final product mixture. The complete set of experiments is summarised in Figure S3 and discussed in detail below.

Neat grinding of a 2:3 molar mixture of $Al(OH)_3$ and $Ca(OH)_2$ (syntheses #3.1–#3.3) leads to the formation of the intermediate hydrogarnet $Ca_3Al_2O_6\cdot 6H_2O$ according to:

$$3\ Ca(OH)_2 + 2\ Al(OH)_{3-} > Ca_3Al_2O_6\ \cdot\ 6H_2O \qquad (5)$$

In syntheses #3.1 and #3.2 (Figure 3, Figure 7, Figure S3), the final reaction mixture contains traces of $Ca(OH)_2$. This indicates that the conversion to hydrogarnet was incomplete. The absence of $Al(OH)_3$ reflections suggests a significant reduction of the corresponding particle size, as should be expected from the above discussion on the grinding effect on pure $Al(OH)_3$

© 2019 The Authors. Published by Wiley-VCH Verlag GmbH & Co. KGaA

(Figure 7). Consistent with these findings, the diffraction data for synthesis #3.3, which refer to a shorter grinding time, contain reflections of both reactant phases indicating an incomplete reaction. A quantity of gypsum was subsequently added to the above-mentioned intermediate mixtures, and grinding was continued for: 5 min for synthesis #3.2) and 30 min for syntheses #3.1 and #3.3. This additional grinding step evidenced further consumption of $Ca(OH)_2$ to form hydrogarnet. Finally, a molar equivalent of water was added to each mixture, and the third grinding step was performed. In each case, trace quantities of gypsum were observed alongside the dominant ettringite product phase.

In contrast, in experiments with the first step involving the neat pre-grinding of $CaSO_4 \cdot 2H_2O$ and $Al(OH)_3$ (synthesis #3.4) or that of $CaSO_4 \cdot 2H_2O$ and $Ca(OH)_2$ (synthesis #3.5), the stepwise addition of all other reactants led to the final product consisting of ettringite and all used reactants. These results confirm that co-grinding of $Al(OH)_3$ and $Ca(OH)_2$ (syntheses #3.1–#3.3) is crucial for the achievement of the increased reaction conversion.

The single grinding of individual reactants reveals their behaviour under mechanochemical treatment. The particle size of $Al(OH)_3$ reduces significantly, and the crystallinity decreases after 60 min grinding by up to 60% and remains constant by further grinding. In contrast, the crystallinity of individually ground $Ca(OH)_2$ or $CaSO_4 \cdot 2H_2O$ remains stable upon prolonged grinding.

The three-step procedures offered new insights into the interactions of reactant phases during mechanosyntheses. Notably, $Al(OH)_3$ and $Ca(OH)_2$ form hydrogarnet in the absence of $CaSO_4 \cdot 2H_2O$ (synthesis #3). If these two reactants are ground in presence of $CaSO_4 \cdot 2H_2O$ for up to 120 min (synthesis #2), the reflections of $Al(OH)_3$ and $Ca(OH)_2$ gradually disappear without hydrogarnet being formed (Figure 5). Their states and transformation products remain unclear. However, the specific interaction of $Al(OH)_3$ and $Ca(OH)_2$ during the grinding seems to be a pre-requisite for the successful formation of ettringite in high yields.

Appropriate analysis of non-crystalline metastable states is needed to obtain information about proposed amorphous intermediates. Further research is needed to decipher the interaction between $Al(OH)_3$ and $Ca(OH)_2$ during the ettringite mechanosynthesis, the existence of their interim phases or the evidenceof their states.

3. Conclusion

An environmentally friendly mechanochemical synthesis of ettringite was developed which combines the advantages of a high conversion/short reaction time (94% in 2 h) with no CO_2 release or waste water production and the need for product separation compared to conventional wet-chemical industrial synthesis. Insights into the reaction mechanism were obtained through the investigation of one-, two- and three-step mechanochemical procedures using different sequences of reactant combinations relying on product characterization by powder X-ray diffraction and granulometric analysis. The neat pre-grinding of the solid educts is crucial for a high conversion to ettringite. The process investigated in this work ensures 94% conversion to ettringite after 2 h . This high conversion seems to be critically dependent on the neat pre-grinding of $Al(OH)_3$ (accompanied by a considerable crystallinity loss and particle size reduction) in the presence of $Ca(OH)_2$ turned out to.

Acknowledgement

We are grateful for funding from the Excellence Initiative of the German Research Foundation (DFG project: GSC 1013) and the Graduate School of Analytical Sciences Adlershof (SALSA). The support from Fundação para a Ciência e a Tecnologia (Portugal) (FCT project: PEst-OE/QUI/UI0100/2013) is also gratefully acknowledged. We thank Heidi Marx (BAM, Berlin) for the laser granulometric analyses.

Conflict of Interest

The authors declare no conflict of interest.

Keywords: Ettringite · mechanochemistry · sustainability · X-ray diffraction

[1] V. Kasselouri, P. Tsakiridis, C. Malami, B. Georgali, C. Alexandridou, *Cem. Concr. Res.* **1995**, *25*, 1726–1736.
[2] Y. J. Liu, Y. M. Xu, C. L. Geng, *Adv. Mater. Res.* **2012**, *368–373*, 478–484.
[3] W. Lerch, *Proceedings-American Society for Testing and Materials.* **1946**, *46*, 1252–1297.
[4] F. W. Locher, W. Richartz, S. Sprung, *ZGK.* **1980**, *33*, 271–277.
[5] M. Collepardi, G. Baldini, M. Pauri, M. Corradi, *J. Am. Ceram. Soc.* **1979**, *62*, 33–35.
[6] M. Alexander, A. Bertron, N. De Belie, *Performance of Cement-Based Materials in Aggressive Aqueous Environments*, Springer, **2013**.
[7] M. Chrysochoou, D. Dermatas, *J. Hazard. Mater.* **2006**, *136*, 20–33.
[8] M. Zhang, E. J. Reardon, *Environ. Sci. Technol.* **2003**, *37*, 2947–2952.
[9] G. J. McCarthy, D. J. Hassett, J. A. Bender, *MRS Proceedings.* **1991**, *245*, 129–140.
[10] S. C. B. Myneni, S. J. Traina, T. J. Logan, G. A. Waychunas, *Environ. Sci. Technol.* **1997**, *31*, 1761–1768.
[11] M. L. D. Gougar, B. E. Scheetz, D. M. Roy, *Waste Manage.* **1996**, *16*, 295–303.
[12] X. Guo, H. Shi, *Mater. Struct.* **2017**, *50*, 245.
[13] Q. Zhang, F. Saito, *Powder Technol.* **2000**, *107*, 43–47.
[14] G. Möschner, B. Lothenbach, J. Rose, A. Ulrich, R. Figi, R. Kretzschmar, *Geochim. Cosmochim. Acta.* **2008**, *72*, 1–18.
[15] A. Emanuelson, S. Hansen, *Cem. Concr. Res.* **1997**, *27*, 1167–1177.
[16] R. Buhlert, H.-J. Kuzel, *ZKG Int.* **1971**, *2*, 83–85.
[17] V. Albino, R. Cioffi, M. Marroccoli, L. Santoro, *J. Hazard. Mater.* **1996**, *51*, 241–252.
[18] R. Allmann, *Chimia.* **1970**, *24*, 99–108.
[19] H. F. W. Taylor in *Hydrated aluminate, ferrite and sulfate phases, Vol. 6*, Thomas Telford, **1997**, 157–186.
[20] N. B. Milestone, Y. Bai, P. R. Borges, N. C. Collier, J. P. Gorce, L. E. Gordon, A. Setiadi, C. A. Utton, Q. Z. Zhou, *Scientific Basis for Nuclear Waste Management XXIX.* **2006**, *932*, 673–680.
[21] J. Lehmkuhl, A. D. Fendel, H. Bings in *Mineralischer Füllstoff und Baustoff-Additiv auf Basis von Calciumaluminiumsulfat und deren Herstellung und Verwendung*, Vol. DE196 11 454A1, Google Patents, **1997**, 6.
[22] A. E. Moore, H. F. W. Taylor, *Acta Crystallogr. Sect. B* **1970**, *B 26*, 386–393.

© 2019 The Authors. Published by Wiley-VCH Verlag GmbH & Co. KGaA

[23] H. Poellmann, S. Auer, H. J. Kuzel, R. Wenda, *Cem. Concr. Res.* **1993**, *23*, 422–430.
[24] H. Poellmann, H. J. Kuzel, R. Wenda, *Cem. Concr. Res.* **1990**, *20*, 941–947.
[25] L. H. Zhong, J. Qu, X. W. Li, X. M. He, Q. W. Zhang, *RSC Adv.* **2016**, *6*, 35203–35209.
[26] A. Terzis, S. Filippakis, H. J. Kuzel, H. Burzlaff, *Z. Kristallogr.* **1987**, *181*, 29–34.
[27] M. Collepardi, G. Baldini, M. Pauri, M. Corradi, *Cem. Concr. Res.* **1978**, *8*, 571–580.
[28] I. Odler in *Hydration, Setting and Hardening of Portland Cement, Vol. 6* (Ed. P. C. Hewlett), Butterworth-Heinemann, Oxford, **1998**, 241–297.
[29] Q. Zhou, F. P. Glasser, *Cem. Concr. Res.* **2001**, *31*, 1333–1339.
[30] L. G. Baquerizo, T. Matschei, K. L. Scrivener, *Cem. Concr. Res.* **2016**, *79*, 31–44.
[31] M. Fridrichová, K. Dvořák, K. Kulísek, A. Masárová, K. Havlíčková, *Adv. Mater. Res.* **2014**, *1000*, 55–58.
[32] E. T. Carlson, H. A. Berman, *J. Res. NBS A Phys. Ch.* **1960**, *64*, 333–341.
[33] F. Goetz-Neunhoeffer, J. Neubauer, P. Schwesig, *Cem. Concr. Res.* **2006**, *36*, 65–70.
[34] E. Álvarez-Ayuso, H. W. Nugteren, *Water Res.* **2005**, *39*, 65–72.
[35] J. Stroh, N. Z. Ali, C. Maierhofer, F. Emmerling, *ACS Omega.* **2019**, *4* 7734–7737.
[36] P. M. Carmona-Quiroga, M. T. Blanco-Varela, *Cem. Concr. Res.* **2013**, *52*, 140–148.
[37] M. B. J. Atkinson, D. K. Bucar, A. N. Sokolov, T. Friscic, C. N. Robinson, M. Y. Bilal, N. G. Sinada, A. Chevannes, L. R. MacGillivray, *Chem. Commun. (Camb.)* **2008**, 5713–5715.
[38] P. Balaz, M. Achimovicova, M. Balaz, P. Billik, Z. Cherkezova-Zheleva, J. M. Criado, F. Delogu, E. Dutkova, E. Gaffet, F. J. Gotor, R. Kumar, I. Mitov, T. Rojac, M. Senna, A. Streletskii, K. Wieczorek-Ciurowa, *Chem. Soc. Rev.* **2013**, *42*, 7571–7637.
[39] T. Friscic, *Chem. Soc. Rev.* **2012**, *41*, 3493–3510.
[40] A. L. Garay, A. Pichon, S. L. James, *Chem. Soc. Rev.* **2007**, *36*, 846–855.
[41] S. L. James, C. J. Adams, C. Bolm, D. Braga, P. Collier, T. Friscic, F. Grepioni, K. D. M. Harris, G. Hyett, W. Jones, A. Krebs, J. Mack, L. Maini, A. G. Orpen, I. P. Parkin, W. C. Shearouse, J. W. Steed, D. C. Waddell, *Chem. Soc. Rev.* **2012**, *41*, 413–447.
[42] G. Mi, F. Saito, M. Hanada, *Powder Technol.* **1997**, *93*, 77–81.
[43] A. V. Trask, D. A. Haynes, W. D. S. Motherwell, W. Jones, *Chem. Commun. (Camb.)* **2006**, 51–53.
[44] C. P. Xu, S. De, A. M. Balu, M. Ojeda, R. Luque, *Chem. Commun. (Camb.)* **2015**, *51*, 6698–6713.
[45] Q. Zhang, F. Saito, *Adv. Powder Technol.* **2012**, *23*, 523–531.
[46] L. Batzdorf, F. Fischer, M. Wilke, K. J. Wenzel, F. Emmerling, *Angew. Chem. Int. Ed.* **2015**, *54*, 1799–1802; *Angew. Chem.* **2015**, *127*, 1819–1822.
[47] L. Batzdorf, N. Zientek, D. Rump, F. Fischer, M. Maiwald, F. Emmerling, *J. Mol. Struct.* **2017**, *1133*, 18–23.
[48] M. K. Beyer, H. Clausen-Schaumann, *Chem. Rev. (Washington, DC, U.S.).* **2005**, *105*, 2921–2948.
[49] E. H. H. Chow, F. C. Strobridge, T. Friscic, *Chem. Commun. (Camb.)* **2010**, *46*, 6368–6370.
[50] F. Fischer, A. Heidrich, S. Greiser, S. Benemann, K. Rademann, F. Emmerling, *Cryst. Growth Des.* **2016**, *16*, 1701–1707.
[51] F. Fischer, G. Scholz, S. Benemann, K. Rademann, F. Emmerling, *CrystEngComm.* **2014**, *16*, 8272–8278.
[52] Y. H. Huang, W. S. Lo, Y. W. Kuo, W. J. Chen, C. H. Lin, F. K. Shieh, *Chem. Commun. (Camb.)* **2017**, *53*, 5818–5821.
[53] H. Kulla, S. Greiser, S. Benemann, K. Rademann, F. Emmerling, *Molecules.* **2016**, *21*, 917.
[54] D. Matoga, M. Oszajca, M. Molenda, *Chem. Commun. (Camb.)* **2015**, *51*, 7637–7640.
[55] M. Pascu, A. Ruggi, R. Scopelliti, K. Severin, *Chem. Commun. (Camb.)* **2013**, *49*, 45–47.
[56] A. Beillard, X. Bantreil, T.-X. Métro, J. Martinez, F. Lamaty, *Green Chem.* **2018**, *20*, 964–968.
[57] S. Gupta, T. Kobayashi, I. Z. Hlova, J. F. Goldston, M. Pruski, V. K. Pecharsky, *Green Chem.* **2014**, *16*, 4378–4388.
[58] C. Mottillo, Y. Lu, M.-H. Pham, M. J. Cliffe, T.-O. Do, T. Friščić, *Green Chem.* **2013**, *15*, 2121–2131.
[59] P. Balaz, E. Dutkova, *Miner. Eng.* **2009**, *22*, 681–694.
[60] V. V. Boldyrev, *Solid State Ionics.* **1993**, *63–5*, 537–543.
[61] V. V. Boldyrev, K. Tkacova, *J. Mater. Synth. Process.* **2000**, *8*, 121–132.
[62] A. Nasser, U. Mingelgrin, *Appl. Clay Sci.* **2012**, *67–68*, 141–150.
[63] P. Scherrer, *Nachrichten von der Gesellschaft der Wissenschaften zu Göttingen, Mathematisch-Physikalische Klasse.* **1918**, *1918*, 98–100.
[64] B. D. Cullity, *Elements of X-Ray diffraction*, Addison-Wesley Publishing Company Inc., Phillippines, **1978**.
[65] H. P. Klug, L. E. Alexander, *X-ray diffraction procedures: For polycrystalline and amorphous materials*, Wiley, **1974**.
[66] A. Tonejc, M. Stubicar, A. M. Tonejc, K. Kosanovic, B. Subotic, I. Smit, *J. Mater. Sci. Lett.* **1994**, *13*, 519–520.
[67] U. Steinike, H. Geissler, H. P. Hennig, K. Jancke, J. Jedamzik, U. Kretzschmar, U. Bollmann, *Z. Anorg. Allg. Chem.* **1990**, *590*, 213–221.
[68] V. Scalise, G. Scholz, E. Kemnitz, *J. Solid State Chem.* **2016**, *243*, 154–161.
[69] T. C. Alex, R. Kumar, S. K. Roy, S. P. Mehrotra, *Powder Technol.* **2014**, *264*, 105–113.
[70] T. C. Alex, R. Kumar, S. K. Roy, S. P. Mehrotra, *Light Metals* **2012**, *2012*, 15–19.
[71] K. J. D. MacKenzie, J. Temuujin, K. Okada, *Thermochim. Acta.* **1999**, *327*, 103–108.
[72] L. Ahrem, G. Scholz, R. Bertram, E. Kemnitz, *J. Phys. Chem. C.* **2016**, *120*, 9236–9244.

Manuscript received: June 17, 2019
Revised manuscript received: July 4, 2019

© 2019 The Authors. Published by Wiley-VCH Verlag GmbH & Co. KGaA